

# Adversarial Virtual Exemplar Learning for Label-Frugal Satellite Image Change Detection

Hichem Sahbi<sup>1</sup>

Sebastien Deschamps<sup>1,2</sup>

<sup>1</sup> Sorbonne University, CNRS, LIP6, F-75005, Paris, France

<sup>2</sup>Therisis Thales, France

---

◆

---

## Abstract

Satellite image change detection aims at finding occurrences of targeted changes in a given scene taken at different instants. This task is highly challenging due to the acquisition conditions and also to the subjectivity of changes. In this paper, we investigate satellite image change detection using active learning. Our method is interactive and relies on a question & answer model which asks the oracle (user) questions about the most informative display (dubbed as virtual exemplars), and according to the user's responses, updates change detections. The main contribution of our method consists in a novel adversarial model that allows frugally probing the oracle with only the most representative, diverse and uncertain virtual exemplars. The latter are learned to challenge the most the trained change decision criteria which ultimately leads to a better re-estimate of these criteria in the following iterations of active learning. Conducted experiments show the out-performance of our proposed adversarial display model against other display strategies as well as the related work.

## 1 INTRODUCTION

Automatic satellite image change detection consists in finding occurrences of *relevant* changes in a given area at an instant  $t_1$  w.r.t. the same area at an earlier instant  $t_0$ . This task is useful in different applications including remote sensing damage assessment after natural hazards (tornadoes, flash-floods, etc.) in order to prioritize disaster response and rescues [2], [3]. Change detection is also known to be highly challenging as observed scenes are subject to many irrelevant changes due to sensors, occlusions, radiometric variations and shadows, weather conditions as well as scene content. Early change detection solutions were based on simple comparisons of multi-temporal signals, via image differences and thresholding, vegetation indices, principal component and change vector analyses [5]–[8]. Other solutions require preliminary preprocessing techniques that mitigate the effect of irrelevant changes by correcting radiometric variations, occlusions, and by estimating the parameters of sensors for registration, etc. [10], [11], [13], [14], [35] or consider these irrelevant changes as a part of statistical appearance modeling [9], [12], [15]–[20].

Among the existing change detection methods, those based on statistical machine learning are particularly effective. However, the success of these methods is bound to the availability of large labeled training sets that comprehensively capture the huge variability in irrelevant changes as well as the user's targeted relevant changes [1], [4]. In practice, labeled sets are scarce and even when available, their labeling may not reflect the user's subjectivity and intention. Several alternative solutions seek to make machine learning methods frugal and less (labeled) data-hungry [23], [32] including few shot [21] and self-supervised learning [33]; however, these methods are agnostic to the users' intention. Other solutions, based on active learning [22], [25]–[31], [101], are rather more suitable where users label very few examples of relevant and irrelevant

changes according to their intention, prior to train and retrain user-dedicated change detection criteria.

In this paper, we devise a novel iterative satellite image change detection solution based on a question & answer model that frugally queries the intention of the user (oracle), and updates change detection results accordingly. These queries are restricted *only* to the most informative subset of exemplars (also referred to as virtual displays) which are *learned* instead of being sampled from the *fixed* pool of unlabeled data. The informativeness of exemplars is modeled with a conditional probability distribution that measures how relevant is a given exemplar in the learned displays given the pool of unlabeled data. Two novel adversarial losses are also introduced in order to learn the display — with the most diverse, representative, and ambiguous exemplars — that challenge the most the previously trained change detection criteria resulting into a better re-estimation of these criteria at the subsequent iterations of change detection. While being adversarial, the two proposed losses are conceptually different from generative adversarial networks (GANs) [34]; GANs aim at producing fake data that mislead the trained discriminators whilst our proposed adversarial losses seek to generate the most informative data for further annotations. In other words, the proposed framework allows to sparingly probe the oracle only on the most representative, diverse and uncertain exemplars that challenge the most the current discriminator, and eventually lead to more accurate ones in the following iterations of change detection. Achieved experiments corroborate these findings and show the effectiveness of our *exemplar and display learning* models against comparative methods.

## 2 PROPOSED METHOD

Let’s consider  $\mathcal{I} = \{\mathbf{x}_i = (p_i, q_i)\}_{i=1}^n \subset \mathbb{R}^d$  as a collection of aligned patch pairs taken from two satellite images captured at two different instants  $t_0, t_1$ , and let  $\mathcal{Y} = \{\mathbf{y}_1, \dots, \mathbf{y}_n\} \subset \{-1, +1\}$  be the underlying unknown labels. Our goal is to train a classifier  $f : \mathcal{I} \rightarrow \{-1, +1\}$  that predicts the unknown labels in  $\{\mathbf{y}_i\}_i$  with  $\mathbf{y}_i = +1$  if the patch  $q_i$  corresponds to a “change” w.r.t. the underlying patch  $p_i$ , and  $\mathbf{y}_i = -1$  otherwise. Training  $f$  requires a subset of hand-labeled data obtained from an oracle. As obtaining these labels is usually highly expensive, the design of  $f$  should be *label-frugal* while being as accurate as possible.

### 2.1 Interactive change detection

Our change detection algorithm is built upon a question & answer iterative process which consists in (i) submitting the *most informative patch pairs* to query their labels from an oracle, and (ii) updating a classifier  $f$  accordingly. In the sequel of this paper, the subset of informative images is dubbed as *display*. Let  $\mathcal{D}_t \subset \mathcal{I}$  be a display shown to the oracle at iteration  $t$ , and  $\mathcal{Y}_t$  as the unknown labels of  $\mathcal{D}_t$ ; considering a random display  $\mathcal{D}_0$ , we train our change detection criteria iteratively (for  $t \in \{0, \dots, T - 1\}$ ) according to the subsequent steps

1/ Probe the oracle with  $\mathcal{D}_t$  to obtain  $\mathcal{Y}_t$ , and train a decision function  $f_t(\cdot)$  on  $\cup_{k=0}^t (\mathcal{D}_k, \mathcal{Y}_k)$ ; the latter corresponds to a support vector machine (SVM) trained on top of graph convolution network features [133].

2/ Select the subsequent display  $\mathcal{D}_{t+1} \subset \mathcal{I} \setminus \cup_{k=0}^t \mathcal{D}_k$ . A strategy that *bruteforces* all the possible displays  $\mathcal{D} \subset \mathcal{I} \setminus \cup_{k=0}^t \mathcal{D}_k$ , trains the associated classifiers  $f_{t+1}(\cdot)$  on  $\mathcal{D} \cup_{k=0}^t \mathcal{D}_k$ , and maintains the display with the highest accuracy is combinatorial and clearly intractable. Besides, collecting labels on each of these displays is also out of reach. In this work, we consider instead display selection strategies, based on active learning, which are rather more tractable; nonetheless, these display strategies should be carefully designed as many of them are equivalent to (or worse than)

basic display strategies that select data uniformly randomly (see for instance [101] and references therein).

Our proposed display model (as the main contribution of this paper) is different from usual sampling strategies (see e.g. Sahbi et al., IGARSS 2021) and relies on synthesizing exemplars, also referred to as virtual exemplars. The latter provide more flexibility (in exploring the uncharted parts of the space of unlabeled data), and these exemplars are found by maximizing diversity, representativity and uncertainty (as shown in the remainder of this paper). Diversity seeks to hallucinate exemplars that allow exploring uncharted parts of  $f_{t+1}(\cdot)$  whereas representativity makes it possible to register the exemplars, as much as possible, to the input data. Finally, ambiguity locally refines the boundaries of the trained classifiers  $f_{t+1}(\cdot)$ .

## 2.2 Virtual exemplar learning: early model

We consider for each sample  $\mathbf{x}_i \in \mathcal{I}$  a membership distribution  $\{\mu_{ik}\}_{k=1}^K$  that measures the *conditional* probability of assigning  $\mathbf{x}_i$  to  $K$ -virtual exemplars; the latter constitute the subsequent display  $\mathcal{D}_{t+1}$ . The proposed method defines  $\mathcal{D}_{t+1}$  (rewritten for short and in a matrix form as  $\mathbf{D}$ ) together with  $\{\mu_{ik}\}_{i,k}$  by minimizing the following constrained objective function

$$\begin{aligned} \min_{\mathbf{D}; \mu \in \Omega} \quad & \text{tr}(\mu d(\mathbf{D}, \mathbf{X})) + \alpha \left[ \frac{1}{n} \mathbf{1}_n^\top \mu \right] \log \left[ \frac{1}{n} \mathbf{1}_n^\top \mu \right]^\top \\ & + \beta \text{tr}(f(\mathbf{D})^\top \log f(\mathbf{D})) + \gamma \text{tr}(\mu^\top \log \mu), \end{aligned} \quad (1)$$

here  $\Omega = \{\mu : \mu \geq 0; \mu \mathbf{1}_K = \mathbf{1}_n\}$ ,  $\mathbf{1}_K$ ,  $\mathbf{1}_n$  denote two vectors of  $K$  and  $n$  ones respectively,  $^\top$  is the matrix transpose operator,  $\mu \in \mathbb{R}^{n \times K}$  is a learned matrix whose  $i$ -th row corresponds to the conditional probability of assigning  $\mathbf{x}_i$  to each of the  $K$ -virtual exemplars, and  $\log$  is applied entrywise. In Eq. 1,  $d(\mathbf{D}, \mathbf{X}) \in \mathbb{R}^{K \times n}$  is the matrix of the euclidean distances between input data in  $\mathbf{X}$  and the virtual exemplars in  $\mathbf{D}$  whereas  $f(\mathbf{D}) \in \mathbb{R}^{2 \times K}$  is a scoring matrix whose columns correspond to the softmax of the learned SVM  $f_t(\cdot)$  (and its complement) applied to the  $K$ -virtual exemplars. The first term in Eq. 1, rewritten as  $\sum_i \sum_k \mu_{ik} \|\mathbf{x}_i - \mathbf{D}_k\|_2^2$ , measures how representative are the virtual exemplars  $\{\mathbf{D}_k\}_k$  w.r.t. the training samples  $\mathbf{X}$ . The second term (equal to  $\sum_k [\frac{1}{n} \sum_{i=1}^n \mu_{ik}] \log [\frac{1}{n} \sum_{i=1}^n \mu_{ik}]$ ) captures the *diversity* of the generated virtual data as the entropy of the probability distribution of the underlying memberships; this measure is minimal when input data are assigned to different virtual exemplars, and vice-versa. The third criterion (equivalent to  $\sum_k \sum_c [f_c(\mathbf{D})]_k^\top [\log f_c(\mathbf{D})]_k$ ) measures the *ambiguity* (or uncertainty) in  $\mathcal{D}_{t+1}$  as the entropy of the scoring function; it reaches its smallest value when virtual exemplars in  $\mathcal{D}_{t+1}$  are evenly scored w.r.t different classes. The fourth term acts as a regularizer which considers that, without any a priori on the three other terms, the conditional probability distribution  $\{\mu_{ik}\}_k$  on each input data is uniform. As shown subsequently, this term also helps obtaining a closed form solution. Finally, we consider equality and inequality constraints which guarantee that the membership of each input sample  $\mathbf{x}_i$  to the virtual exemplars forms a conditional probability distribution.

## 2.3 Virtual exemplar learning: surrogate model

The formulation proposed in the aforementioned section, in spite of being relatively effective (as shown later in experiments), has a downside: it combines heterogeneous terms (entropy and distance based criteria) whose mixing hyperparameters are difficult to optimize<sup>1</sup>. In what

1. This requires trying many settings of these hyperparameters, inducing the underlying displays and labeling them by the oracle. This is clearly out of reach in interactive satellite image change detection as labeling changes/no-changes should be very sparingly and frugally achieved.

follows, we consider a surrogate objective function which considers only homogeneous (distance based) criteria, excepting the regularizer, and this turns out to be more effective as shown later in experiments. With this variant, the virtual exemplars together with their distributions  $\{\mu_{ik}\}_{i,k}$  are now obtained by minimizing the following problem

$$\begin{aligned} \min_{\mathbf{D}; \mu \in \Omega} \quad & \text{tr}(\mu d(\mathbf{D}, \mathbf{X})) + \frac{\alpha}{2} \left\| \frac{1}{n} \mathbf{1}_n^\top \mu - \frac{1}{K} \mathbf{1}_K^\top \right\|_F^2 \\ & + \frac{\beta}{2} \left\| f(\mathbf{D}) - \frac{1}{2} \mathbf{1}_2 \mathbf{1}_K^\top \right\|_F^2 + \gamma \text{tr}(\mu^\top \log \mu), \end{aligned} \quad (2)$$

here  $\|\cdot\|_F$  is the Frobenius norm. The first and fourth terms of the above objective function remain unchanged while the second and third terms, despite being different, *their impact is strictly equivalent when considered separately and positive when combined*. Indeed, the second term, equal to  $\sum_k (\frac{1}{n} \sum_i \mu_{ik} - \frac{1}{K})^2$ , aims at assigning the same probability mass to the virtual exemplars (and this maximizes entropy) whilst the third term, equal to  $\sum_k \sum_c (f_c(\mathbf{D}_k) - \frac{1}{2})^2$ , has also an equivalent behavior w.r.t. its counterpart in Eq. 1, namely, it favors virtual exemplars whose SVM softmax scores are the closest to  $\frac{1}{2}$  (i.e., near the SVM decision boundary), and this also maximizes entropy. This similar behavior is also corroborated through the observed performances on these terms when taken individually<sup>2</sup>; nevertheless, the joint combination of these homogeneous terms (through Eq. 2) provides a more pronounced gain compared to their heterogeneous counterparts (in Eq. 1) as shown later in experiments.

## 2.4 Optimization

**Proposition 1.** The optimality conditions of Eqs. (1) and (2) lead to

$$\begin{aligned} \mu^{(\tau+1)} & := \mathbf{diag}(\hat{\mu}^{(\tau+1)} \mathbf{1}_K)^{-1} \hat{\mu}^{(\tau+1)}, \\ \mathbf{D}^{(\tau+1)} & := \hat{\mathbf{D}}^{(\tau+1)} \mathbf{diag}(\mathbf{1}'_n \mu^{(\tau)})^{-1}, \end{aligned} \quad (3)$$

with  $\hat{\mu}^{(\tau+1)}$ ,  $\hat{\mathbf{D}}^{(\tau+1)}$  being respectively for Eq. (1)

$$\begin{aligned} & \exp\left(-\frac{1}{\gamma} [d(\mathbf{X}, \mathbf{D}^{(\tau)}) + \frac{\alpha}{n} \mathbf{1}_n (\mathbf{1}_K^\top + \log \frac{1}{n} \mathbf{1}_n^\top \mu^{(\tau)})]\right) \\ & \mathbf{X} \mu^{(\tau)} + \beta \sum_c \nabla_v f_c(\mathbf{D}^{(\tau)}) \circ (\mathbf{1}_d [\log f_c(\mathbf{D}^{(\tau)})]' + \mathbf{1}_d \mathbf{1}'_K), \end{aligned} \quad (4)$$

and for Eq. (2)

$$\begin{aligned} & \exp\left(-\frac{1}{\gamma} [d(\mathbf{X}, \mathbf{D}^{(\tau)}) + \frac{\alpha}{n} \mathbf{1}_n (\frac{1}{n} \mathbf{1}_n^\top \mu^{(\tau)} - \frac{1}{K} \mathbf{1}_K^\top)]\right) \\ & \mathbf{X} \mu^{(\tau)} + \beta \sum_c \nabla_v f_c(\mathbf{D}^{(\tau)}) \circ (\mathbf{1}_d [f_c(\mathbf{D}^{(\tau)}) - \frac{1}{2} \mathbf{1}_K^\top]), \end{aligned} \quad (5)$$

here  $\circ$  stands for the Hadamard product and  $\mathbf{diag}(\cdot)$  maps a vector to a diagonal matrix.

In view of space, details of the proof are omitted and result from the optimality conditions of Eq. 1's and Eq. 2's gradients and lagrangians. Note that  $\mu^{(0)}$  and  $\mathbf{D}^{(0)}$  are initially set to random values and, in practice, the procedure converges to an optimal solution (denoted as  $\tilde{\mu}$ ,  $\tilde{\mathbf{D}}$ ) in few iterations. This solution defines the most *relevant* virtual exemplars of  $\mathcal{D}_{t+1}$  (according to criteria in Eqs. 1 or 2) which are used to train the subsequent classifier  $f_{t+1}$  (see also algorithm 1). Note also that  $\alpha$  and  $\beta$  are set in order to make the impact of the underlying terms equally proportional; in other words, inversely proportional to the number of matrix entries intervening in these terms, and this corresponds to  $O(K^{-1})$  for both  $\alpha$  and  $\beta$ . Finally, since  $\gamma$  acts as scaling factor that controls the shape of the exponential function, its setting is iteration-dependent and proportional to the term inside the square brackets of that exponential.

2. This equivalence of performances is also due to the fact that no weighting is necessary when these terms are used individually.

---

**Algorithm 1:** Display selection mechanism
 

---

**Input:** Images in  $\mathcal{I}$ , display  $\mathcal{D}_0 \subset \mathcal{I}$ , budget  $T$ .

**Output:**  $\cup_{t=0}^{T-1} (\mathcal{D}_t, \mathcal{Y}_t)$  and  $\{f_t\}_t$ .

**for**  $t := 0$  **to**  $T - 1$  **do**

$\mathcal{Y}_t \leftarrow \text{oracle}(\mathcal{D}_t)$ ;

$f_t \leftarrow \arg \min_f \text{Loss}(f, \cup_{k=0}^t (\mathcal{D}_k, \mathcal{Y}_k))$ ;

$\tau \leftarrow 0$ ;  $\hat{\mu}^{(0)} \leftarrow \text{random}$ ;  $\mathbf{D}^{(0)} \leftarrow \text{random}$ ;

  Set  $\mu^{(0)}$  and  $\mathbf{D}^{(0)}$  using Eq. (3);

**while**  $(\|\mu^{(\tau+1)} - \mu^{(\tau)}\|_1 + \|\mathbf{D}^{(\tau+1)} - \mathbf{D}^{(\tau)}\|_1 \geq \epsilon$

$\wedge \tau < \text{maxiterations})$  **do**

    Update  $\mu^{(\tau+1)}$  and  $\mathbf{D}^{(\tau+1)}$  using Eq. (3);

$\tau \leftarrow \tau + 1$ ;

$\tilde{\mu} \leftarrow \mu^{(\tau)}$ ;  $\tilde{\mathbf{D}} \leftarrow \mathbf{D}^{(\tau)}$ ;

$\mathcal{D}_{t+1} \leftarrow \{\mathbf{x}_i \in \mathcal{I} \setminus \cup_{k=0}^t \mathcal{D}_k : \mathbf{x}_i \leftarrow \arg \min_{\mathbf{x}} \|\mathbf{x} - \mathbf{D}_k\|_2^2\}_{k=1}^K$ .

---

### 3 EXPERIMENTS

Change detection experiments are conducted on the Jefferson dataset. The latter includes 2,200 aligned patch pairs (of  $30 \times 30$  RGB pixels each) taken from bi-temporal GeoEye-1 satellite images of  $2,400 \times 1,652$  pixels with a spatial resolution of 1.65m/pixel. These images were taken from the area of Jefferson (Alabama) in 2010 and 2011 with many changes (building destruction, etc.) due to tornadoes as well as no-changes (including irrelevant ones as clouds). This dataset includes 2,161 negative pairs (no/irrelevant changes) and only 39 positive pairs (relevant changes), so less than 2% of these data correspond to relevant changes, and this makes their localization very challenging. In our experiments, we split the whole dataset evenly; one half to train our display and learning models while the remaining half to measure accuracy. As changes/no-changes classes are highly off-balanced, we measure accuracy using the equal error rate (EER); smaller EER implies better performances.

#### 3.1 Ablation

We first study the impact of each term of our objective functions separately, and then we consider them jointly and all combined. Note that the regularization term is always kept as it allows to obtain the closed form solutions shown in proposition 1. Table 1 illustrates the impact of these terms where EER performances are shown for each configuration using both the early and the surrogate models respectively. As expected, when using the terms separately, their impact on change detection performances are very similar (and sometimes identical), and this results from their equivalence; put differently, the solution reached by these terms — even though presented in different ways in their respective objective functions — have similar behavior when used separately. However, when jointly combining these terms, their impact is different, and this results from their heterogeneity in Eq. 1 and homogeneity in Eq. 2 which makes the setting of the underlying mixing hyperparameters in the latter configuration easier and also more effective. From these results, we also observe the highest impact of representativity+diversity especially at the earliest iterations of change detection, whilst the impact of ambiguity term raises later in order to locally refine the decision criteria (i.e., once the modes of data distribution become well explored). These EER performances are shown for different sampling percentages defined — at each iteration  $t$  — as  $(\sum_{k=0}^{t-1} |\mathcal{D}_k| / (|\mathcal{I}|/2)) \times 100$  with  $|\mathcal{I}| = 2,200$  and  $|\mathcal{D}_k|$  set to 16.

#### 3.2 Comparison

We also compare our display model w.r.t. other display selection strategies including pool-based methods namely *random search*, *maxmin* and *uncertainty*. Random consists in sampling

| rep   | div | amb | 1     | 2     | 3           | 4           | 5           | 6           | 7           | 8           | 9           | 10          | AUC.         |
|-------|-----|-----|-------|-------|-------------|-------------|-------------|-------------|-------------|-------------|-------------|-------------|--------------|
| ✗     | ✗   | ✓   | 47.81 | 27.29 | 11.15       | 7.97        | 8.18        | 7.31        | 7.97        | 7.94        | 7.50        | 7.90        | 14.10        |
|       |     |     | 47.81 | 18.71 | 11.23       | 7.96        | 8.17        | 7.28        | 7.58        | 7.88        | 7.49        | 7.90        | 13.21        |
| ✗     | ✓   | ✗   | 47.81 | 18.72 | 11.24       | 7.97        | 8.18        | 7.29        | 7.59        | 7.88        | 7.50        | 7.90        | 13.21        |
|       |     |     | 47.81 | 18.71 | 11.23       | 7.96        | 8.17        | 7.28        | 7.58        | 7.88        | 7.49        | 7.90        | 13.21        |
| ✓     | ✗   | ✗   | 47.81 | 35.98 | 16.86       | 6.52        | 4.98        | 2.67        | 2.03        | 1.80        | 1.45        | 1.30        | 12.14        |
|       |     |     | 47.81 | 35.98 | 16.86       | 6.52        | 4.98        | 2.67        | 2.03        | 1.80        | 1.45        | 1.30        | 12.14        |
| ✓     | ✗   | ✓   | 47.81 | 40.40 | 23.86       | 9.56        | 7.65        | 5.75        | 5.47        | 6.12        | 4.40        | 5.72        | 15.67        |
|       |     |     | 47.81 | 36.75 | 29.26       | 8.61        | 4.27        | 2.37        | 2.34        | 1.68        | 1.45        | 1.27        | 13.59        |
| ✗     | ✓   | ✓   | 47.81 | 27.29 | 11.15       | 7.97        | 8.18        | 7.31        | 7.97        | 7.94        | 7.50        | 7.90        | 14.10        |
|       |     |     | 47.81 | 28.94 | 12.39       | 9.12        | 7.05        | 6.94        | 7.05        | 7.09        | 7.25        | 6.93        | 14.06        |
| ✓     | ✓   | ✗   | 47.81 | 29.84 | 17.63       | 6.21        | 4.40        | 2.70        | 1.98        | 1.92        | 1.65        | 1.52        | 11.57        |
|       |     |     | 47.81 | 38.20 | 23.73       | 9.36        | 7.67        | 5.67        | 4.66        | 4.31        | 3.28        | 2.59        | 14.73        |
| ✓     | ✓   | ✓   | 47.81 | 27.61 | 11.76       | 5.74        | 2.95        | 2.39        | 1.89        | 1.61        | 1.55        | 1.34        | 10.47        |
|       |     |     | 47.81 | 32.56 | <b>9.88</b> | <b>4.54</b> | <b>2.71</b> | <b>2.00</b> | <b>1.56</b> | <b>1.21</b> | <b>1.10</b> | <b>1.08</b> | <b>10.44</b> |
| Samp% |     |     | 1.45  | 2.90  | 4.36        | 5.81        | 7.27        | 8.72        | 10.18       | 11.63       | 13.09       | 14.54       | -            |

TABLE 1

This table shows an ablation study of our display model. Here rep, amb and div stand for representativity, ambiguity and diversity respectively. For each configuration of “rep”, “amb” and “div”, the results are shown in two rows corresponding to the early and the surrogate display models respectively. These results are also shown for different iterations  $t = 0, \dots, T - 1$  (Iter) and the underlying sampling rates (Samp) again defined as  $(\sum_{k=0}^{t-1} |\mathcal{D}_k| / (|\mathcal{I}|/2)) \times 100$ . The AUC (Area Under Curve) corresponds to the average of EERs across iterations.

displays from the pool of unlabeled data whereas uncertainty aims at choosing, from the same pool, the most ambiguous data, i.e., whose SVM scores are the closest to zero. Maxmin seeks to greedily select the most distinct data in  $\mathcal{D}_{t+1}$ ; each sample in  $\mathbf{x}_i \in \mathcal{D}_{t+1} \subset \mathcal{I} \setminus \cup_{k=0}^t \mathcal{D}_k$  is chosen by *maximizing its minimum distance w.r.t.*  $\cup_{k=0}^t \mathcal{D}_k$ . We further compare our display model against the model in (Sahbi et al., IGARSS 2021) which assigns marginal probability measures (instead of conditional ones) to the unlabeled data and selects the data in the subsequent display with the highest probability values. Finally, we report performances using a fully-supervised setting that considers the entire training set (whose labels are taken from the ground-truth) in order to learn a single monolithic classifier, and the EER of the latter is considered as a lower bound. The EER performances of these settings are shown in Figure 1 through different iterations and sampling rates, as well as the aforementioned display selection strategies. From these results, most of the comparative methods are powerless to spot the rare class (i.e., changes) sufficiently well. Indeed, while random and maxmin capture the diversity during the early stages of interactive change detection they are less effective in refining the learned decision functions whilst uncertainty overcomes this issues, it lacks diversity. The display selection strategy in (Sahbi et al., IGARSS 2021) captures diversity and refines better the learned classifiers, however, it suffers from the rigidity of the selected displays (especially at the early iterations) which are taken from a fixed pool of training data. In contrast, our proposed display models gather the advantages of the aforementioned methods while they also allow learning more flexible displays that further enhance change detection performances through different iterations. Besides, the surrogate model leads to an extra gain in performances especially at mid and late iterations of change detection which particularly correspond to highly frugal learning regimes.

## 4 CONCLUSION

We introduce in this paper a new interactive satellite image change detection algorithm. The proposed solution is based on active learning and consists in learning both a classifier and a subset of data (referred to as virtual display) resulting into a more flexible model. These virtual

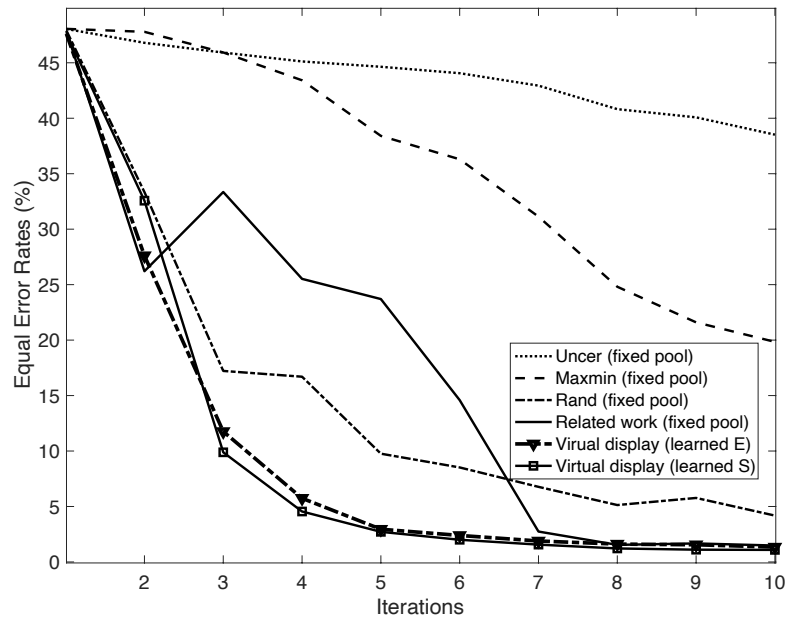


Fig. 1. This figure shows a comparison of different sampling strategies w.r.t. different iterations (Iter) and the underlying sampling rates in table 1 (Samp). Here “Uncer” and “Rand” stand for uncertainty and random sampling respectively while “learned E”, “learned S” correspond to the proposed early and surrogate display models respectively. Note that fully-supervised learning achieves an EER of 0.94%. Related work stands for the method in (Sahbi et al., IGARSS 2021); see again section 3.2 for more details.

displays are obtained by maximizing their representativity, diversity and also their uncertainty, and this provides a more effective adversarial model that challenges the current trained classifiers leading to more effective subsequent ones. All these findings are corroborated through extensive experiments conducted on the challenging task of interactive satellite image change detection which show the out-performance of the proposed virtual display models against different baselines and pool-based methods as well as the related work.

## REFERENCES

- [1] P. Vo and H. Sahbi. “Transductive kernel map learning and its application to image annotation.” *BMVC*. 2012.
- [2] D. Brunner, G. Lemoine, and L. Bruzzone, Earthquake damage assessment of buildings using vhr optical and sar imagery, *IEEE Trans. Geosc. Remote Sens.*, vol. 48, no. 5, pp. 2403–2420, 2010.
- [3] H. Gokon, J. Post, E. Stein, S. Martinis, A. Twele, M. Muck, C. Geiss, S. Koshimura, and M. Matsuoka, A method for detecting buildings destroyed by the 2011 tohoku earthquake and tsunami using multitemporal terrasars-x data, *GRSL*, vol. 12, no. 6, pp. 1277–1281, 2015.
- [4] Q. Oliveau and H. Sahbi. “Learning attribute representations for remote sensing ship category classification.” *IEEE JSTARS* 10.6 (2017): 2830-2840.
- [5] J. Deng, K. Wang, Y. Deng, and G. Qi, PCA-based land-use change detection and analysis using multitemporal and multisensor satellite data, *IJRS*, vol. 29, no. 16, pp. 4823–4838, 2008.
- [6] R. Radke, S. Andra, O. Al-Kofahi, and B. Roysam, Image change detection algorithms: A systematic survey, *IEEE Trans. on Im Proc*, vol. 14, no. 3, pp. 294–307, 2005.
- [7] S. Liu, L. Bruzzone, F. Bovolo, M. Zanetti, and P. Du, Sequential spectral change vector analysis for iteratively discovering and detecting multiple changes in hyperspectral images, *TGRS*, 53(8), pp. 4363–4378, 2015.
- [8] G. Chen, G. J. Hay, L. M. Carvalho, and M. A. Wulder, Object-based change detection, *IJRS*, vol. 33, no. 14, pp. 4434–4457, 2012.
- [9] H. Sahbi. “Interactive satellite image change detection with context-aware canonical correlation analysis.” *IEEE GRSL*, (14)5, 2017.
- [10] J. Zhu, Q. Guo, D. Li, and T. C. Harmon, Reducing mis-registration and shadow effects on change detection in wetlands, *Photogrammetric Engineering & Remote Sensing*, vol. 77, no. 4, pp. 325–334, 2011.

- [11] A. Fournier, P. Weiss, L. Blanc-Fraud, and G. Aubert, A contrast equalization procedure for change detection algorithms: applications to remotely sensed images of urban areas, In ICPR, 2008
- [12] H. Sahbi. "Relevance feedback for satellite image change detection." IEEE ICASSP, 2013.
- [13] Carlotto, Detecting change in images with parallax, In Society of Photo-Optical Instrumentation Engineers, 2007
- [14] S. Leprince, S. Barbot, F. Ayoub, and J.-P. Avouac, Automatic and precise orthorectification, coregistration, and subpixel correlation of satellite images, application to ground deformation measurements, TGRS, vol. 45, no. 6, pp. 1529–1558, 2007.
- [15] Pollard, Comprehensive 3d change detection using volumetric appearance modeling, Phd, Brown University, 2009.
- [16] A. A. Nielsen, The regularized iteratively reweighted mad method for change detection in multi-and hyperspectral data, IEEE Transactions on Image processing, vol. 16, no. 2, pp. 463–478, 2007.
- [17] C. Wu, B. Du, and L. Zhang, Slow feature analysis for change detection in multispectral imagery, TGRS, vol. 52, no. 5, pp. 2858–2874, 2014
- [18] N. Bourdis, D. Marraud and H. Sahbi. "Constrained optical flow for aerial image change detection." in IEEE IGARSS, 2011.
- [19] J. Im, J. Jensen, and J. Tullis, Object-based change detection using correlation image analysis and image seg, IJRS, 29(2), 399–423, 2008.
- [20] N. Bourdis, D. Marraud, and H. Sahbi, Spatio-temporal interaction for aerial video change detection, in IGARSS, 2012, pp. 2253–2256
- [21] Vinyals et al., Matching networks for one shot learning. 2016.
- [22] Dasgupta, Sanjoy. "Analysis of a greedy active learning strategy." Advances in neural information processing systems 17 (2004).
- [23] H. Sahbi. "Coarse-to-fine deep kernel networks." IEEE ICCV-W, 2017.
- [24] Burr, Settles. "Active learning." Synthesis Lectures on Artificial Intelligence and Machine Learning 6.1 (2012).
- [25] Tianxu et al., An Active Learning Approach with Uncertainty, Representativeness, and Diversity,
- [26] Joshi et al., Multi-class active learning for image classification. 2009.
- [27] Settles & Craven. An analysis of active learning strategies for sequence labeling tasks. 2008.
- [28] Houlshby et al., Bayesian active learning for classification and preference learning. 2011.
- [29] Campbell & Broderick, Automated scalable Bayesian inference via Hilbert coresets. 2019.
- [30] Gal et al., Deep bayesian active learning with image data. 2017
- [31] Pang et al., Meta-Learning Transferable Active Learning Policies by Deep Reinforcement Learning
- [32] M. Jiu and H. Sahbi. "Laplacian deep kernel learning for image annotation." IEEE ICASSP, 2016.
- [33] A. Kolesnikov, X. Zhai, L. Beyer. Revisiting Self-Supervised Visual Representation Learning. IEEE/CVF CVPR, 2019, pp. 1920-1929
- [34] Creswell, Antonia, et al. "Generative adversarial networks: An overview." IEEE Signal Processing Magazine 35.1 (2018): 53-65.
- [35] N. Bourdis, D. Marraud and H. Sahbi. "Camera pose estimation using visual servoing for aerial video change detection." IEEE IGARSS 2012.
- [36] Jia Deng, Wei Dong, Richard Socher, Li-Jia Li, Kai Li, and Li Fei-Fei. Imagenet: A large-scale hierarchical image database. In 2009 IEEE conference on computer vision and pattern recognition, pages 248–255. Ieee, 2009
- [37] H. Sahbi and N. Boujemaa. "Robust matching by dynamic space warping for accurate face recognition." Proceedings 2001 International Conference on Image Processing (Cat. No. 01CH37205). Vol. 1. IEEE, 2001.
- [38] Sabrina Tollari, Philippe Mulhem, Marin Ferecatu, Hervé Glotin, Marcin Detyniecki, Patrick Gallinari, H. Sahbi, and Zhong-Qiu Zhao. "A comparative study of diversity methods for hybrid text and image retrieval approaches." In Workshop of the Cross-Language Evaluation Forum for European Languages, pp. 585-592. Springer, Berlin, Heidelberg, 2008.
- [39] Ashish Vaswani, Noam Shazeer, Niki Parmar, Jakob Uszkoreit, Llion Jones, Aidan N. Gomez, Lukasz Kaiser, Illia Polosukhin. Attention Is All You Need. arXiv:1706.03762. 2017.
- [40] Krizhevsky, Alex, Ilya Sutskever, and Geoffrey E. Hinton. "Imagenet classification with deep convolutional neural networks." Advances in neural information processing systems 25 (2012): 1097-1105.
- [41] A. Mazari and H. Sahbi. "MLGCN: Multi-Laplacian graph convolutional networks for human action recognition." The British Machine Vision Conference (BMVC). 2019.
- [42] Szegedy, Christian, et al. "Rethinking the inception architecture for computer vision." Proceedings of the IEEE conference on computer vision and pattern recognition. 2016.
- [43] M. Ferecatu and H. Sahbi. "TELECOM ParisTech at ImageClefphoto 2008: Bi-Modal Text and Image Retrieval with Diversity Enhancement." CLEF (Working Notes). 2008.
- [44] Szegedy, Christian, et al. "Inception-v4, inception-resnet and the impact of residual connections on learning." Thirty-first AAAI conference on artificial intelligence. 2017.
- [45] Clemens-Alexander Brust, Christoph Kading, and Joachim Denzler. Active learning for deep object detection. arXiv preprint arXiv:1809.09875, 2018.
- [46] Mei Wang and Weihong Deng. Deep visual domain adaptation: A survey. Neurocomputing, 312:135–153, 2018.

- [47] Connor Shorten and Taghi M Khoshgoftaar. A survey on image data augmentation for deep learning. *Journal of Big Data*, 6(1):1–48, 2019.
- [48] H. Sahbi. "Lightweight Connectivity In Graph Convolutional Networks For Skeleton-Based Recognition." 2021 IEEE International Conference on Image Processing (ICIP). IEEE, 2021.
- [49] Keze Wang, Liang Lin, Xiaopeng Yan, Ziliang Chen, Dongyu Zhang, and Lei Zhang. Cost-effective object detection: Active sample mining with switchable selection criteria. CoRR, abs/1807.00147, 2018.
- [50] Vladimir Haltakov, Christian Unger, and Slobodan Ilic. Framework for generation of synthetic ground truth data for driver assistance applications. In *German conference on pattern recognition*, pages 323–332. Springer, 2013.
- [51] H. Sahbi, Jean-Yves Audibert, Jaonary Rabarisoa, and Renaud Keriven. "Context-dependent kernel design for object matching and recognition." In 2008 IEEE Conference on Computer Vision and Pattern Recognition, pp. 1-8. IEEE, 2008.
- [52] Begum Demir, Claudio Persello, and Lorenzo Bruzzone. Batch-mode active-learning methods for the interactive classification of remote sensing images. *IEEE Transactions on Geoscience and Remote Sensing*, 49(3):1014–1031, 2010.
- [53] H. Sahbi, Jean-Yves Audibert, and Renaud Keriven. "Graph-cut transducers for relevance feedback in content based image retrieval." 2007 IEEE 11th International Conference on Computer Vision. IEEE, 2007.
- [54] Krause, Andreas, and Carlos Guestrin. "Nonmyopic active learning of gaussian processes: an exploration-exploitation approach." *Proceedings of the 24th international conference on Machine learning*. 2007.
- [55] M. Jiu and H. Sahbi. "Deep representation design from deep kernel networks." *Pattern Recognition* 88 (2019): 447-457.
- [56] Robert Pinsler, Jonathan Gordon, Eric T. Nalisnick, and Jose Miguel Hernandez-Lobato. Bayesian batch active learning as sparse subset approximation. In Hanna M. Wallach, Hugo Larochelle, Alina Beygelzimer, Florence d'Alche Buc, Emily B. Fox, and Roman Garnett, editors, *NeurIPS*, pages 6356–6367, 2019.
- [57] S. Thiemert, H. Sahbi, and M. Steinebach. "Applying interest operators in semi-fragile video watermarking." *Security, Steganography, and Watermarking of Multimedia Contents VII*. Vol. 5681. SPIE, 2005.
- [58] Ricardo BC Prudencio and Teresa B Ludermir. Selective generation of training examples in active meta-learning. *International Journal of Hybrid Intelligent Systems*, 5(2):59–70, 2008.
- [59] Hiranmayi Ranganathan, Hemanth Venkateswara, Shayok Chakraborty, and Sethuraman Panchanathan. Deep active learning for image classification. In 2017 IEEE International Conference on Image Processing (ICIP), pages 3934–3938. IEEE, 2017.
- [60] Snell, Jake, Kevin Swersky, and Richard S. Zemel. "Prototypical networks for few-shot learning." arXiv preprint arXiv:1703.05175 (2017).
- [61] H. Sahbi. "Imageclef annotation with explicit context-aware kernel maps." *International Journal of Multimedia Information Retrieval* 4.2 (2015): 113-128.
- [62] Sener, Ozan, and Silvio Savarese. "Active learning for convolutional neural networks: A core-set approach." arXiv preprint arXiv:1708.00489 (2017).
- [63] David D Lewis and William A Gale. A sequential algorithm for training text classifiers. In *SIGIR'94*, pages 3–12. Springer, 1994.
- [64] H. Sahbi. "Learning laplacians in chebyshev graph convolutional networks." *Proceedings of the IEEE/CVF International Conference on Computer Vision*. 2021.
- [65] Xin Li and Yuhong Guo. Adaptive active learning for image classification. In *CVPR*, pages 859–866. IEEE Computer Society, 2013.
- [66] Ajay J. Joshi, Fatih Porikli, and Nikolaos Papanikolopoulos. Multi-class active learning for image classification. In *CVPR*, pages 2372–2379. IEEE Computer Society, 2009.
- [67] L. Wang and H. Sahbi. "Bags-of-daglets for action recognition." 2014 IEEE International Conference on Image Processing (ICIP). IEEE, 2014.
- [68] Burr Settles. Active learning literature survey. *Computer Sciences Technical Report 1648*, University of Wisconsin–Madison, 2009
- [69] Frank Olken. Random sampling from databases. PhD thesis, University of California, Berkeley, 1993.
- [70] Maria E Ramirez-Loaiza, Manali Sharma, Geet Kumar, and Mustafa Bilgic. Active learning: an empirical study of common baselines. *Data mining and knowledge discovery*, 31(2):287–313, 2017.
- [71] Andreas Kirsch, Joost van Amersfoort, and Yarin Gal. Batchbald: Efficient and diverse batch acquisition for deep bayesian active learning, 2019.
- [72] H. Sahbi. "CNRS-TELECOM ParisTech at ImageCLEF 2013 Scalable Concept Image Annotation Task: Winning Annotations with Context Dependent SVMs." *CLEF (Working Notes)*. 2013.
- [73] Stefan Depeweg, Jose-Miguel Hernandez-Lobato, Finale Doshi-Velez, and Steffen Udluft. Decomposition of uncertainty in bayesian deep learning for efficient and risk-sensitive learning. In *International Conference on Machine Learning*, pages 1184–1193. PMLR, 2018.
- [74] Simon Tong and Daphne Koller. Support vector machine active learning with applications to text classification. *Journal of machine learning research*, 2(Nov):45–66, 2001.
- [75] Sahbi, H., and N. Boujemaa. "Robust face recognition using dynamic space warping." *International Workshop on Biometric Authentication*. Springer, Berlin, Heidelberg, 2002.

- [76] Ashish Kapoor, Kristen Grauman, Raquel Urtasun, and Trevor Darrell. Active learning with gaussian processes for object categorization. In 2007 IEEE 11th International Conference on Computer Vision, pages 1–8. IEEE, 2007.
- [77] Sachin Ravi and Hugo Larochelle. Meta-learning for batch mode active learning. 2018. In URL <https://openreview.net/forum>, 2018.
- [78] Kunkun Pang, Mingzhi Dong, Yang Wu, and Timothy Hospedales. Meta-learning transferable active learning policies by deep reinforcement learning. arXiv preprint arXiv:1806.04798, 2018.
- [79] Yi Yang, Zhigang Ma, Feiping Nie, Xiaojun Chang, and Alexander G. Hauptmann. Multi-class active learning by uncertainty sampling with diversity maximization. *Int. J. Comput. Vis.*, 113(2):113–127, 2015.
- [80] S. Thiemert, H. Sahbi, and M. Steinebach. "Using entropy for image and video authentication watermarks." *Security, Steganography, and Watermarking of Multimedia Contents VIII*. Vol. 6072. SPIE, 2006.
- [81] Christoph Mayer and Radu Timofte. Adversarial sampling for active learning. In *Proceedings of the IEEE/CVF Winter Conference on Applications of Computer Vision*, pages 3071–3079, 2020.
- [82] Dwarikanath Mahapatra, Behzad Bozorgtabar, Jean-Philippe Thiran, and Mauricio Reyes. Efficient active learning for image classification and segmentation using a sample selection and conditional generative adversarial network, 2019.
- [83] H. Sahbi and N. Boujemaa. "Coarse-to-fine support vector classifiers for face detection." *Object recognition supported by user interaction for service robots*. Vol. 3. IEEE, 2002.
- [84] Jia-Jie Zhu and Jose Bento. Generative adversarial active learning. *CoRR*, abs/1702.07956, 2017.
- [85] Longlong Jing and Yingli Tian. Self-supervised visual feature learning with deep neural networks: A survey. *IEEE transactions on pattern analysis and machine intelligence*, 2020.
- [86] Yong Cheng Wu. Active learning based on diversity maximization. In *Applied Mechanics and Materials*, volume 347, pages 2548–2552. *Trans Tech Publ*, 2013.
- [87] Sharat Agarwal, Himanshu Arora, Saket Anand, and Chetan Arora. Contextual diversity for active learning. In *European Conference on Computer Vision*, pages 137–153. Springer, 2020.
- [88] Yarin Gal. *Uncertainty in Deep Learning*. PhD thesis, University of Cambridge, 2016.
- [89] Yarin Gal and Zoubin Ghahramani. Dropout as a bayesian approximation: Representing model uncertainty in deep learning, 2016.
- [90] H. Sahbi. Coarse-to-fine support vector machines for hierarchical face detection. Diss. PhD thesis, Versailles University, 2003.
- [91] Donggeun Yoo and In So Kweon. Learning loss for active learning. In *Proceedings of the IEEE/CVF Conference on Computer Vision and Pattern Recognition*, pages 93–102, 2019.
- [92] Patrick Hemmer, Niklas Kuhl, and Jakob Schoffer. Deal: Deep evidential active learning for image classification. In *2020 19th IEEE International Conference on Machine Learning and Applications (ICMLA)*, pages 865–870, 2020.
- [93] Jordan T Ash, Chicheng Zhang, Akshay Krishnamurthy, John Langford, and Alekh Agarwal. Deep batch active learning by diverse, uncertain gradient lower bounds. arXiv preprint arXiv:1906.03671, 2019.
- [94] N. Boujemaa, F. Fleuret, V. Gouet, and H. Sahbi. "Visual content extraction for automatic semantic annotation of video news." In the proceedings of the SPIE Conference, San Jose, CA, vol. 6. 2004.
- [95] Yoram Baram, Ran El Yaniv, and Kobi Luz. Online choice of active learning algorithms. *Journal of Machine Learning Research*, 5(Mar):255–291, 2004.
- [96] Ksenia Konyushkova, Raphael Sznitman, and Pascal Fua. Learning active learning from data. arXiv preprint arXiv:1703.03365, 2017.
- [97] H. Sahbi. "Misalignment resilient cca for interactive satellite image change detection." *2016 23rd International Conference on Pattern Recognition (ICPR)*. IEEE, 2016.
- [98] Sheng-Jun Huang, Rong Jin, and Zhi-Hua Zhou. Active learning by querying informative and representative examples. In John D. Lafferty, Christopher K. I. Williams, John Shawe-Taylor, Richard S. Zemel, and Aron Culotta, editors, *NIPS*, pages 892–900. Curran Associates, Inc., 2010.
- [99] T. Napoléon and H. Sahbi. "From 2D silhouettes to 3D object retrieval: contributions and benchmarking." *EURASIP Journal on Image and Video Processing 2010 (2010)*: 1-17.
- [100] Naoki Abe. Query learning strategies using boosting and bagging. *Proc. of ICML98*, pages 1–9, 1998.
- [101] Burr Settles. "Active learning." *Synthesis Lectures on Artificial Intelligence and Machine Learning 6.1 (2012)*.
- [102] X. Li and H. Sahbi. "Superpixel-based object class segmentation using conditional random fields." *2011 IEEE International Conference on Acoustics, Speech and Signal Processing (ICASSP)*. IEEE, 2011.
- [103] Sutton, Richard S., and Andrew G. Barto. *Reinforcement learning: An introduction*. MIT press, 2018.
- [104] Jin, C., Allen-Zhu, Z., Bubeck, S., & Jordan, M.I. (2018). Is Q-learning provably efficient?. arXiv preprint arXiv:1807.03765.
- [105] Dosovitskiy, Alexey, et al. "An image is worth 16x16 words: Transformers for image recognition at scale." arXiv preprint arXiv:2010.11929 (2020).
- [106] Carl Doersch, Abhinav Gupta, Alexei A. Efros. Unsupervised Visual Representation Learning by Context Prediction, arXiv:1505.05192, 2015.
- [107] M. Jiu and H. Sahbi. "Semi supervised deep kernel design for image annotation." *2015 IEEE International Conference on Acoustics, Speech and Signal Processing (ICASSP)*. IEEE, 2015.

- [108] Culotta, Aron, and Andrew McCallum. "Reducing labeling effort for structured prediction tasks." *AAAI*. Vol. 5. 2005.
- [109] M. Jiu and H. Sahbi. "Deep kernel map networks for image annotation." 2016 IEEE International Conference on Acoustics, Speech and Signal Processing (ICASSP). IEEE, 2016.
- [110] Atwood, J., Towsley, D.: Diffusion-convolutional neural networks. In: *Advances in Neural Information Processing Systems*. pp. 1993–2001 (2016)
- [111] Bruna, J., Zaremba, W., Szlam, A., LeCun, Y.: Spectral networks and locally connected networks on graphs. arXiv preprint arXiv:1312.6203 (2013)
- [112] Chen, J., Zhu, J., Song, L.: Stochastic training of graph convolutional networks with variance reduction. arXiv preprint arXiv:1710.10568 (2017)
- [113] Chen, J., Ma, T., Xiao, C.: Fastgcn: fast learning with graph convolutional networks via importance sampling. arXiv preprint arXiv:1801.10247 (2018)
- [114] H. Sahbi and N. Boujemaa. "From coarse to fine skin and face detection." *Proceedings of the eighth ACM international conference on Multimedia*. 2000.
- [115] Dai, H., Kozareva, Z., Dai, B., Smola, A., Song, L.: Learning steady-states of iterative algorithms over graphs. In: *International Conference on Machine Learning*. pp. 1114–1122 (2018)
- [116] Defferrard, M., Bresson, X., Vandergheynst, P.: Convolutional neural networks on graphs with fast localized spectral filtering. In: *Advances in neural information processing systems*. pp. 3844–3852 (2016)
- [117] H. Sahbi and F. Fleuret. *Kernel methods and scale invariance using the triangular kernel*. Diss. INRIA, 2004.
- [118] Gao, H., Wang, Z., Ji, S.: Large-scale learnable graph convolutional networks. In: *Proceedings of the 24th ACM SIGKDD International Conference on Knowledge Discovery & Data Mining*. pp. 1416–1424. ACM (2018)
- [119] Gori, M., Monfardini, G., Scarselli, F.: A new model for learning in graph domains. In: *Proceedings. 2005 IEEE International Joint Conference on Neural Networks, 2005*. vol. 2, pp. 729–734. IEEE (2005)
- [120] Hamilton, W., Ying, Z., Leskovec, J.: Inductive representation learning on large graphs. In: *Advances in Neural Information Processing Systems*. pp. 1024–1034 (2017)
- [121] Henaff, M., Bruna, J., LeCun, Y.: Deep convolutional networks on graph-structured data. arXiv preprint arXiv:1506.05163 (2015)
- [122] H. Sahbi and F. Fleuret. *Scale-invariance of support vector machines based on the triangular kernel*. Diss. INRIA, 2002.
- [123] Huang, W., Zhang, T., Rong, Y., Huang, J.: Adaptive sampling towards fast graph representation learning. In: *Advances in Neural Information Processing Systems*. pp. 4558–4567 (2018)
- [124] Kipf, T.N., Welling, M.: Semi-supervised classification with graph convolutional networks. arXiv preprint arXiv:1609.02907 (2016)
- [125] Levie, R., Monti, F., Bresson, X., Bronstein, M.M.: Cayleynets: Graph convolutional neural networks with complex rational spectral filters. *IEEE Transactions on Signal Processing* **67**(1), 97–109 (2018)
- [126] Li, R., Wang, S., Zhu, F., Huang, J.: Adaptive graph convolutional neural networks. In: *Thirty-Second AAAI Conference on Artificial Intelligence* (2018)
- [127] L. Wang and H. Sahbi. "Nonlinear cross-view sample enrichment for action recognition." *European Conference on Computer Vision*. Springer, Cham, 2014.
- [128] Li, Y., Tarlow, D., Brockschmidt, M., Zemel, R.: Gated graph sequence neural networks. arXiv preprint arXiv:1511.05493 (2015)
- [129] Wu, Z., Pan, S., Chen, F., Long, G., Zhang, C., Yu, P.S.: A comprehensive survey on graph neural networks. arXiv preprint arXiv:1901.00596 (2019)
- [130] Zhang, J., Shi, X., Xie, J., Ma, H., King, I., Yeung, D.Y.: Gaan: Gated attention networks for learning on large and spatiotemporal graphs. arXiv preprint arXiv:1803.07294 (2018)
- [131] M. Ferencat and H. Sahbi. "Multi-view object matching and tracking using canonical correlation analysis." 2009 16th IEEE International Conference on Image Processing (ICIP). IEEE, 2009.
- [132] T. Ma, J. Chen, and C. Xiao, "Constrained generation of semantically valid graphs via regularizing variational autoencoders," in *Proc. of NeurIPS, 2018*, pp. 7110–7121.
- [133] H. Sahbi. "Learning Connectivity with Graph Convolutional Networks." 2020 25th International Conference on Pattern Recognition (ICPR). IEEE, 2021.
- [134] S. Pan, R. Hu, G. Long, J. Jiang, L. Yao, and C. Zhang, "Adversarially regularized graph autoencoder for graph embedding." in *Proc. of IJCAI 2018*, pp. 2609–2615.